

Multimode high-sensitive optical $\text{YVO}_4:\text{Ln}^{3+}$ nanothermometers ($\text{Ln}^{3+} = \text{Eu}^{3+}, \text{Dy}^{3+}, \text{Sm}^{3+}$) using charge transfer band features

I.E. Kolesnikov^{a,b,*}, M.A. Kurochkin^a, E.V. Golyeva^c, D.V. Mamonova^a, A.A. Kalinichev^a, E.Yu. Kolesnikov^d, E. Lähderanta^b

^a St. Petersburg State University, Universitetskaya nab. 7-9, 199034, St. Petersburg, Russia

^b LUT University, Skinnarilankatu 34, 53850, Lappeenranta, Finland

^c Peter the Great St. Petersburg Polytechnic University, Polytechnicheskaya str. 29, 195251, St. Petersburg, Russia

^d Volga State University of Technology, Lenin sqr. 3, 424000, Yoshkar-Ola, Russia

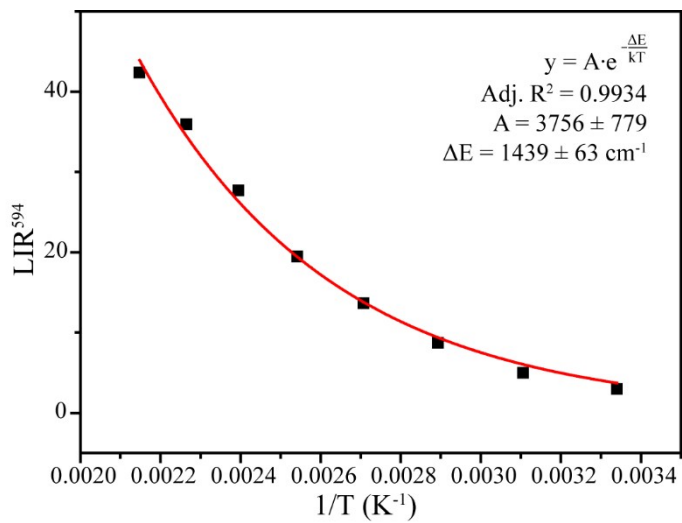


Figure S1. Evolution of LIR⁵⁹⁴ as a function of temperature for YVO₄:Eu³⁺ 1 at.% nanoparticles.

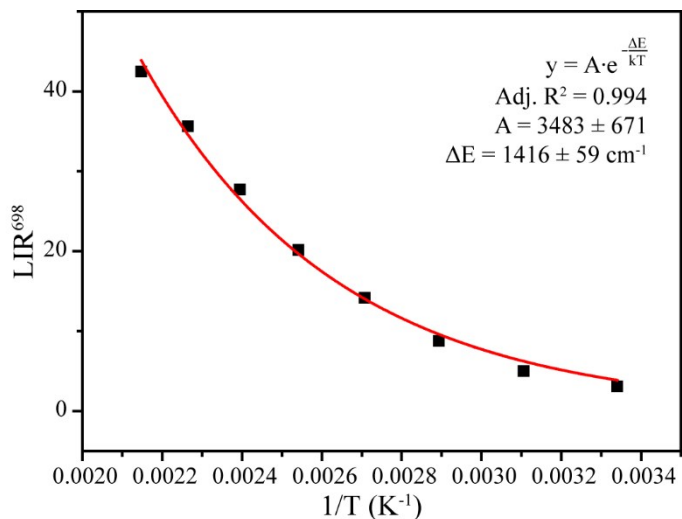


Figure S2. Evolution of LIR⁶⁹⁸ as a function of temperature for YVO₄:Eu³⁺ 1 at.% nanoparticles.

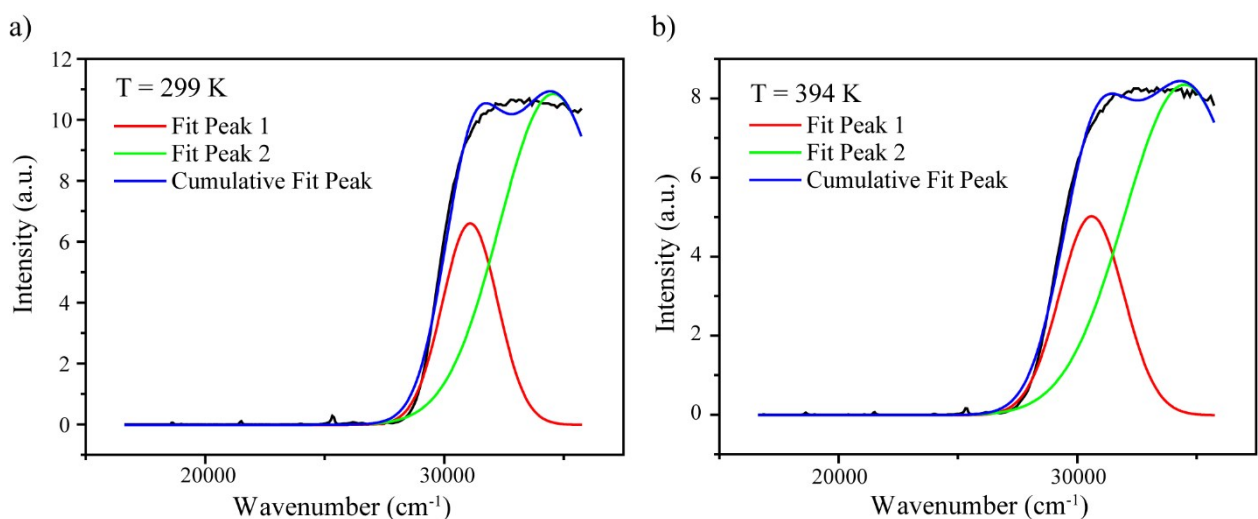


Figure S3. Deconvolution procedure of CTB of $\text{YVO}_4:\text{Eu}^{3+}$ 1 at.% nanoparticles a) $T = 299 \text{ K}$ and b) $T = 394 \text{ K}$.

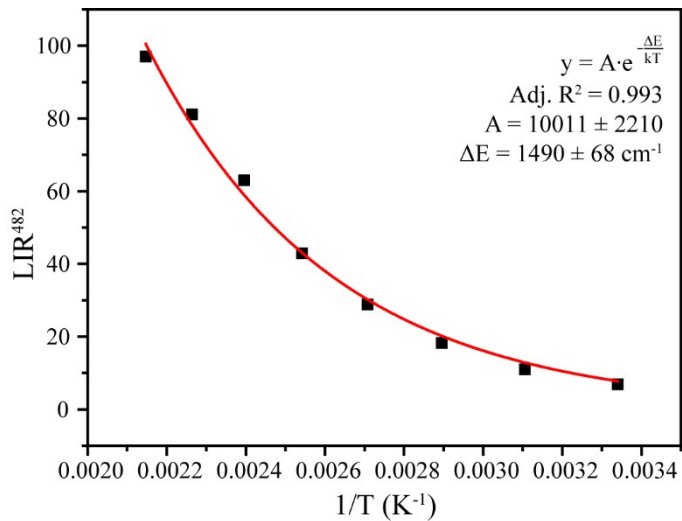


Figure S4. Evolution of LIR^{482} as a function of temperature for $\text{YVO}_4:\text{Dy}^{3+}$ 1 at.% nanoparticles.

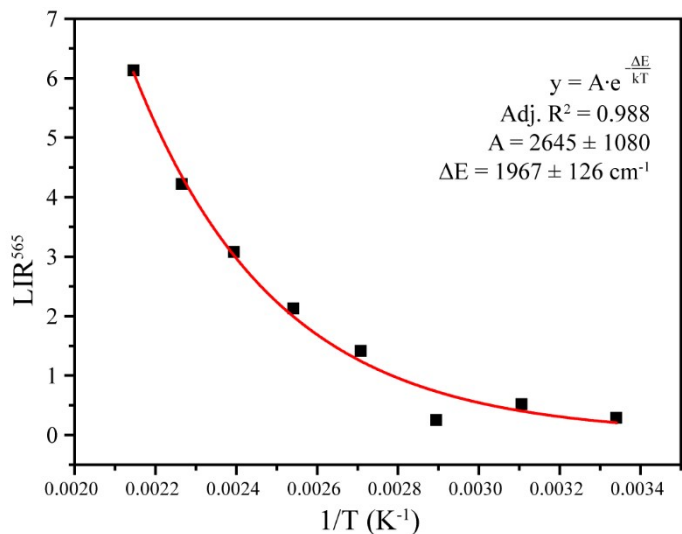


Figure S5. Evolution of LIR^{565} as a function of temperature for $\text{YVO}_4:\text{Sm}^{3+}$ 1 at.% nanoparticles.

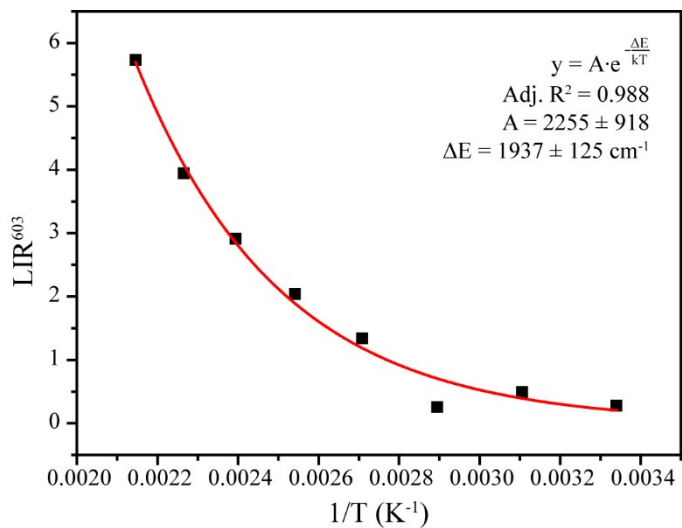


Figure S6. Evolution of LIR⁶⁰³ as a function of temperature for YVO₄:Sm³⁺ 1 at.% nanoparticles.

Table S1. Comparison of LIR-based sensitivities calculated from different transitions for YVO₄:Ln³⁺ (Ln³⁺ = Eu³⁺, Dy³⁺, Sm³⁺) nanoparticles.

Material	Transition	S _r (%K ⁻¹)@299K
YVO ₄ :Eu ³⁺ 1 at.%	⁵ D ₀ - ⁷ F ₁ (594 nm)	2.31
	⁵ D ₀ - ⁷ F ₂ (619 nm)	2.23
	⁵ D ₀ - ⁷ F ₄ (698 nm)	2.27
YVO ₄ :Dy ³⁺ 1 at.%	⁴ F _{9/2} - ⁶ H _{15/2} (482 nm)	2.39
	⁴ F _{9/2} - ⁶ H _{13/2} (572 nm)	2.37
YVO ₄ :Sm ³⁺ 1 at.%	⁴ G _{5/2} - ⁶ H _{5/2} (565 nm)	3.16
	⁴ G _{5/2} - ⁶ H _{7/2} (603 nm)	3.11
	⁴ G _{5/2} - ⁶ H _{9/2} (646 nm)	3.09